Lower Bounds for the Error in Nitsche's Method for the Navier–Stokes Equations With Slip Boundary Conditions

Ingeborg Gjerde, Simula L. Ridgway Scott, University of Chicago

July 1, 2021

Abstract

We investigate lower bounds for the error in Nitsche's Method to implement slip boundary conditions for flow problems in domains with curved boundaries. We study approximations of the normal and tangent vectors when using a polygonal approximation of the domain. For both approaches, we give lower bounds for the error that give an upper bound on the best convergence rate that can be achieved for a polygonal approximation of a curved boundary. Our results support the idea that extra mesh refinement near a curved boundary can mitigate the polygonal domain approximation error.

The implementation of slip boundary conditions for Stokes' equations on a curved boundary introduces unique difficulties not seen for scalar problems. In a recent paper [5], we proved upper bounds for the error when using Nitsche's Method to impose slip boundary conditions on curved boundaries. Here we consider corresponding lower bounds in order to clarify whether the results of [5] are sharp. We are only partially successful in that in one important case there is a gap between the upper and lower bounds.

In an application, we consider flow past a cylinder as in [5].

1 Navier–Stokes equations

Suppose that (\mathbf{u}, p) is a solution of the stationary Navier–Stokes equations in a domain $\Omega \subset \mathbb{R}^d$ containing an obstacle with boundary $\Gamma \subset \partial \Omega$:

$$-\nu \Delta \mathbf{u} + \mathbf{u} \cdot \nabla \mathbf{u} + \nabla p = \mathbf{0} \text{ in } \Omega,$$

$$\nabla \cdot \mathbf{u} = 0 \text{ in } \Omega,$$
 (1)

where ν is the kinematic viscosity, together with boundary conditions

$$\mathbf{u} = \mathbf{g} \text{ on } \partial \Omega \backslash \Gamma, \quad \mathbf{u} \cdot \mathbf{n} = 0 \text{ on } \Gamma,$$
 (2)

together with Navier's friction boundary condition [7]

$$\beta \mathbf{u} \cdot \boldsymbol{\tau}^k = -\nu \mathbf{n}^t (\nabla \mathbf{u} + \nabla \mathbf{u}^t) \boldsymbol{\tau}^k, \quad k = 1, 2,$$
(3)

where τ^i are orthogonal tangent vectors and β is a constant. The following is proved in [5].

Lemma 1.1 Suppose that $\mathbf{u} \in H^2(\Omega)^d$, $p \in H^1(\Omega)$, and $\mathbf{v} \in H^1(\Omega)^d$. Then

$$\int_{\Omega} (-\nu \Delta \mathbf{u} + \nabla p) \cdot \mathbf{v} \, d\mathbf{x} = \int_{\Omega} \frac{\nu}{2} \mathcal{D}(\mathbf{u}) : \mathcal{D}(\mathbf{v}) - p \nabla \cdot \mathbf{v} \, d\mathbf{x} - \oint_{\partial \Omega} (\nu \mathcal{D}(\mathbf{u}) - pI) \mathbf{v} \cdot \mathbf{n} \, ds, \quad (4)$$

where $\mathcal{D}(\mathbf{v}) = \nabla \mathbf{v} + \nabla \mathbf{v}^t$ and \mathbf{n} is the outward normal to $\partial \Omega$.

1.1 Proof of Lemma 1.1

There are two parts to (4). The one involving p is a consequence of the divergence theorem

$$\int_{\Omega} \nabla \cdot \mathbf{w} \, d\mathbf{x} = \oint_{\partial \Omega} \mathbf{w} \cdot \mathbf{n} \, ds,$$

applied to $\mathbf{w} = p\mathbf{v}$, since $\nabla \cdot (p\mathbf{v}) = \nabla p \cdot \mathbf{v} + p \nabla \cdot \mathbf{v}$. Similarly, let $\mathbf{w} = \mathcal{D}(\mathbf{u})\mathbf{v}$. We claim that, if $\nabla \cdot \mathbf{u} = 0$,

$$\nabla \cdot (\mathcal{D}(\mathbf{u})\mathbf{v}) = (\Delta \mathbf{u}) \cdot \mathbf{v} + \frac{1}{2}\mathcal{D}(\mathbf{u}) : \mathcal{D}(\mathbf{v}). \tag{5}$$

To prove this, we expand using indices:

$$\nabla \cdot (\mathcal{D}(\mathbf{u})\mathbf{v}) = \sum_{i} (\mathcal{D}(\mathbf{u})\mathbf{v})_{i,i} = \sum_{ij} (\mathcal{D}(\mathbf{u})_{ij}\mathbf{v}_{j})_{,i}$$

$$= \sum_{ij} (\mathcal{D}(\mathbf{u})_{ij}\mathbf{v}_{j,i} + \mathcal{D}(\mathbf{u})_{ij,i}\mathbf{v}_{j})$$

$$= \sum_{ij} \mathcal{D}(\mathbf{u})_{ij}\mathbf{v}_{j,i} + \sum_{ij} (\mathbf{u}_{i,ji} + \mathbf{u}_{j,ii})\mathbf{v}_{j}$$

$$= \mathcal{D}(\mathbf{u}) : \nabla \mathbf{v}^{t} + \mathbf{v} \cdot \nabla(\nabla \cdot \mathbf{u}) + \Delta \mathbf{u} \cdot \mathbf{v} = \mathcal{D}(\mathbf{u}) : \nabla \mathbf{v}^{t} + \Delta \mathbf{u} \cdot \mathbf{v}.$$
(6)

But the symmetry of $\mathcal{D}(\mathbf{u})$ implies that

$$\mathcal{D}(\mathbf{u}): \nabla \mathbf{v}^t = \mathcal{D}(\mathbf{u})^t: \nabla \mathbf{v} = \mathcal{D}(\mathbf{u}): \nabla \mathbf{v}$$

so that $\mathcal{D}(\mathbf{u}) : \mathcal{D}(\mathbf{v}) = \mathcal{D}(\mathbf{u}) : \nabla \mathbf{v}^t + \mathcal{D}(\mathbf{u}) : \nabla \mathbf{v} = 2\mathcal{D}(\mathbf{u}) : \nabla \mathbf{v}^t$. Thus

$$\nabla \cdot (\mathcal{D}(\mathbf{u})\mathbf{v}) = \frac{1}{2}\mathcal{D}(\mathbf{u}) : \mathcal{D}(\mathbf{v}) + \Delta \mathbf{u} \cdot \mathbf{v},$$

proving (5). A second application of the divergence theorem confirms (4).

1.2 Variational form

The corresponding weak formulation of the stationary Navier–Stokes equations is

$$\frac{\nu}{2}(\mathcal{D}(\mathbf{u}), \mathcal{D}(\mathbf{v})) - (p, \nabla \cdot \mathbf{v}) + \oint_{\Gamma} \beta \sum_{i} (\boldsymbol{\tau}^{i} \cdot \mathbf{v}) (\boldsymbol{\tau}^{i} \cdot \mathbf{u}) \, ds = F(\mathbf{v}) \quad \forall \, \mathbf{v} \in W, \tag{7}$$

where $F(\mathbf{v}) = -(\mathbf{u} \cdot \nabla \mathbf{u}, \mathbf{v})$ and

$$W = \left\{ \mathbf{v} \in H^1(\Omega)^d : \mathbf{v} = \mathbf{0} \text{ on } \partial\Omega \backslash \Gamma, \ \mathbf{v} \cdot \mathbf{n} = 0 \text{ on } \Gamma \right\}.$$

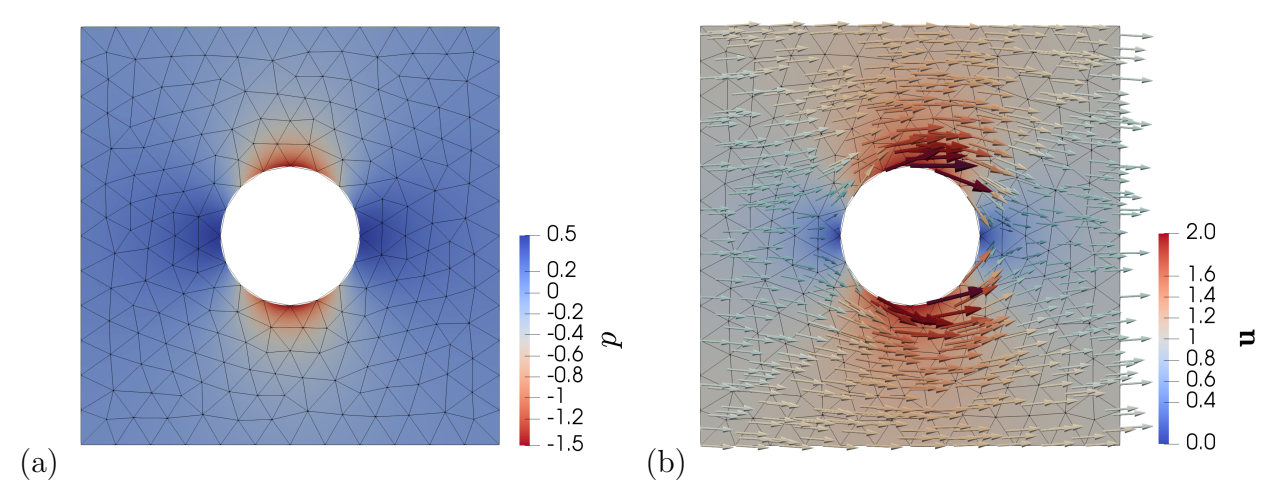


Figure 1: Solution of the Navier–Stokes equation (15) for $\nu=1$ with $\beta=-2$ (potential flow). Plot of (a) pressure p and (b) velocity ${\bf u}$ for potential flow ($\beta=-2$), computed on the indicated coarse mesh. The mesh was generated using gmsh. The computation was done in a box of dimensions 4×4 , and the cylinder of radius 1 is centered in the box. Dirichlet conditions on the boundary of the box were given by the potential flow solution.

2 Potential flow around a cylinder

Potential flow around a cylinder of radius 1 and aligned with the z-axis is given [4] by $\mathbf{u} = \nabla \phi$ where

$$\phi(x,y,z) = \phi(r,\theta,z) = \left(r + \frac{1}{r}\right)\cos\theta = x + \frac{x}{x^2 + y^2}.$$
 (8)

The solution is depicted in Figure 1. The velocity components are given by

$$u_x(x,y,z) = 1 - \frac{x^2 - y^2}{(x^2 + y^2)^2}, \qquad u_y(x,y,z) = \frac{-2xy}{(x^2 + y^2)^2}, \qquad u_z = 0.$$
 (9)

Thus [4] **u** satisfies $\Delta \mathbf{u} = \nabla \Delta p = 0$ and

$$-\nu\Delta\mathbf{u} + \mathbf{u} \cdot \nabla\mathbf{u} + \nabla p = 0,$$

where

$$p = -\frac{1}{2}|\mathbf{u}|^2 = -\frac{1}{2}|\nabla\phi|^2,$$
 (10)

and we have a solution of (1) for any ν .

We can take the normal and tangent vectors on the cylinder to be

$$\mathbf{n} = -(x, y, 0), \quad \boldsymbol{\tau}^1 = (y, -x, 0), \quad \boldsymbol{\tau}^2 = (0, 0, 1).$$

The shear stress can likewise be computed [4], and we find that the shear stress is equal to the tangential velocity on the cylinder. Thus (3) is satisfied for $\beta = -2\nu$.

Thus potential flow for the cylinder provides an exact solution of Navier–Stokes for any Reynolds number for $\beta = -2\nu$, suitable for studying a numerical implementation.

3 Nitsche's method

The variational expression comparable to (7) but allowing $\mathbf{u} \cdot \mathbf{n} \neq 0$ and $\mathbf{v} \cdot \mathbf{n} \neq 0$ is [5]

$$\frac{\nu}{2}(\mathcal{D}(\mathbf{u}), \mathcal{D}(\mathbf{v})) - (p, \nabla \cdot \mathbf{v}) + \oint_{\Gamma} \sum_{k} \beta(\mathbf{u} \cdot \boldsymbol{\tau}^{k})(\mathbf{v} \cdot \boldsymbol{\tau}^{k}) ds
- \oint_{\Gamma} \mathbf{n}^{t} (\nu \mathcal{D}(\mathbf{u}) - pI) \mathbf{n}(\mathbf{n} \cdot \mathbf{v}) ds = F(\mathbf{v})$$
(11)

for all $\mathbf{v} \in H^1(\Omega)^d$, where $F(\mathbf{v}) = -(\mathbf{u} \cdot \mathbf{u}, \mathbf{v})$. Nitsche's method [5] uses the form

$$A((\mathbf{u}, p, \rho), (\mathbf{v}, q, \sigma); \mathbf{n}) = \frac{\nu}{2} (\mathcal{D}(\mathbf{u}), \mathcal{D}(\mathbf{v})) + \oint_{\Gamma} \sum_{k} \beta(\mathbf{u} \cdot \boldsymbol{\tau}^{k}) (\mathbf{v} \cdot \boldsymbol{\tau}^{k}) ds$$

$$- \oint_{\Gamma} \mathbf{n}^{t} (\nu \mathcal{D}(\mathbf{u}) - pI) \mathbf{n} (\mathbf{n} \cdot \mathbf{v}) ds - \oint_{\Gamma} \mathbf{n}^{t} (\nu \mathcal{D}(\mathbf{v}) - qI) \mathbf{n} (\mathbf{n} \cdot \mathbf{u}) ds$$

$$- (p, \nabla \cdot \mathbf{v}) - (q, \nabla \cdot \mathbf{u}) + \int_{\Omega} \rho \, q + \sigma \, p \, d\mathbf{x} + \gamma \oint_{\Gamma} h^{-1} (\mathbf{u} \cdot \mathbf{n}) (\mathbf{v} \cdot \mathbf{n}) \, ds,$$
(12)

where $\rho, \sigma \in \mathbb{R}$, $\gamma > 0$ is a constant that must be chosen sufficiently large and h is a function that indicates the local mesh size. This bilinear form is defined on the restricted space $H_N^1(\Omega)$ defined by

$$H_N^1(\Omega) = \left\{ \mathbf{v} \in H^1(\Omega)^d : \mathbf{v} = \mathbf{0} \text{ on } \partial\Omega \backslash \Gamma, \quad \mathcal{D}(\mathbf{v}) \Big|_{\Gamma} \in L^2(\Gamma)^{d^2} \right\}, \tag{13}$$

and the corresponding pressure space

$$\Pi_N(\Omega) = \left\{ q \in L^2(\Omega) : q \big|_{\Gamma} \in L^2(\Gamma) \right\}. \tag{14}$$

The following is proved in [5].

Lemma 3.1 Suppose that the pair $(\mathbf{u}, p) \in (V \cap H_N^1(\Omega)^d) \times \Pi_N$ solves (7) with the boundary conditions (2) and (3). Then

$$A((\mathbf{u}, p, 0), (\mathbf{v}, q, \sigma); \mathbf{n}, \boldsymbol{\tau}) = F(\mathbf{v})$$
(15)

for all $\mathbf{v} \in H_N^1(\Omega)$, $q \in \Pi_N$, $\sigma \in \mathbb{R}$, and for any h and γ .

The computational approximation of the nonlinear problem (15) involves solving linear variational problems with right-hand-side $F(\mathbf{v}) = -(\mathbf{u} \cdot \nabla \mathbf{u}, \mathbf{v})$ via various techniques. Many automated systems [6] will apply Newton's method automatically just based on the request to solve

$$A_h((\mathbf{u}_h, p, \rho), (\mathbf{v}, q, \sigma)) + \int_{\Omega_h} (\mathbf{u}_h \cdot \nabla \mathbf{u}_h) \cdot \mathbf{v} \, dx = 0$$
 (16)

with the indicated spaces and Dirichlet boundary condition on $\partial \Omega \backslash \Gamma$.

3.1 Polygonal approximations

We approximate the domain Ω by simplicial complexes Ω_h , where the edge lengths of $\partial \Omega_h$ are of order h in size. This is indicated schematically in a figure in [9]. Then conventional finite elements are employed, with the various boundary expressions being approximated by appropriate quantities. In particular, we assume that Ω_h is triangulated with a nondegenerate family of meshes \mathcal{T}_h of maximum simplex size h_{Ω} . We define

$$W_h^k = \left\{ \mathbf{v} \in C(\Omega_h) : \mathbf{v} = \mathbf{0} \text{ on } \Omega_h \backslash \Gamma_h, \ \mathbf{v}|_T \in \mathcal{P}_k(T)^d \ \forall T \in \mathcal{T}_h \right\},$$

$$\Pi_h^k = \left\{ q \in C(\Omega_h) : q|_T \in \mathcal{P}_{k-1}(T)^d \ \forall T \in \mathcal{T}_h \right\}.$$

To define the bilinear form on the polygonal domain, we need to be precise about the normal and tangential vectors. The simplest approach is to take the normal \mathbf{n}_h and tangents $\boldsymbol{\tau}_h^i$ of the polygonal approximate domain Ω_h . We will see that this is sub-optimal.

For $\mathbf{x} \in \Gamma_h$, define $\boldsymbol{\pi}(\mathbf{x}) \in \Gamma$ by projecting orthogonal to Γ_h to get the closest point on Γ , and then define $\mathbf{n}_{\pi}(\mathbf{x}) = \mathbf{n}(\boldsymbol{\pi}(\mathbf{x}))$ to give a continuous "normal" on Γ_h . Similarly, define $\boldsymbol{\tau}_{\pi} = \boldsymbol{\tau}^i \circ \boldsymbol{\pi}$ on Γ_h . We assume that $\boldsymbol{\pi}$ is invertible, which it will be for h sufficiently small. Define, for any set of vectors \mathbf{n} and $\boldsymbol{\tau}^i$,

$$A((\mathbf{u}, p, \rho), (\mathbf{v}, q, \sigma); \mathbf{n}) = a(\mathbf{u}, \mathbf{v}; \mathbf{n}) + b(\mathbf{u}, q; \mathbf{n}) + b(\mathbf{v}, p; \mathbf{n}) + \int_{\Omega_h} \rho \, q + \sigma \, p \, dx, \tag{17}$$

where

$$a(\mathbf{u}, \mathbf{v}; \mathbf{n}) = \frac{\nu}{2} \int_{\Omega_h} \mathcal{D}(\mathbf{u}) : \mathcal{D}(\mathbf{v}) \, dx + \oint_{\Gamma_h} \sum_i \beta(\mathbf{u} \cdot \boldsymbol{\tau}^i) (\mathbf{v} \cdot \boldsymbol{\tau}^i) \, ds$$

$$- \oint_{\Gamma_h} \nu \, \mathbf{n}^t \mathcal{D}(\mathbf{u}) \mathbf{n} \, (\mathbf{n} \cdot \mathbf{v}) \, ds - \oint_{\Gamma_h} \nu \, \mathbf{n}^t \mathcal{D}(\mathbf{v}) \mathbf{n} \, (\mathbf{n} \cdot \mathbf{u}) \, ds + \gamma \oint_{\Gamma_h} h^{-1} (\mathbf{u} \cdot \mathbf{n}) (\mathbf{v} \cdot \mathbf{n}) \, ds,$$
(18)

and

$$b(\mathbf{v}, q; \mathbf{n}) = -(q, \nabla \cdot \mathbf{v})_h + \oint_{\Gamma_h} q(\mathbf{n} \cdot \mathbf{v}) ds$$
(19)

where

$$(p,q)_h = \int_{\Omega_h} p \, q \, dx.$$

Although the form $a(\mathbf{u}, \mathbf{v}; \mathbf{n})$ depends on the tangent vectors $\boldsymbol{\tau}^i$, it is indexed by just \mathbf{n} since the tangent space spanned by $\boldsymbol{\tau}^i$ is the space orthogonal to \mathbf{n} in all cases, as discussed in [5]. We index these two choices of normals (and corresponding tangent vectors) as follows:

$$\mathbf{n}^{i} = \begin{cases} \mathbf{n}_{\pi} & i = 1\\ \mathbf{n}_{h} & i = 2. \end{cases}$$
 (20)

Then the Taylor–Hood approximation [8] finds $\mathbf{u}_h^i \in \mathbf{g}_I + W_h^k$, $p_h^i \in \Pi_h^k$, and $\rho \in \mathbb{R}$ satisfying

$$A((\mathbf{u}_h^i, p_h^i, \rho), (\mathbf{v}, q, \sigma); \mathbf{n}^i) = F(\mathbf{v})$$
(21)

for all $(\mathbf{v}, q, \sigma) \in W_h^k \times \Pi_h^k \times \mathbb{R}$, where \mathbf{g}_I denotes a suitable interpolant of \mathbf{g} .

In [5], the choice $(\mathbf{n}, \boldsymbol{\tau}^k) = (\mathbf{n}_{\pi}, \boldsymbol{\tau}_{\pi}^k)$ is called the Nitsche method with projected normals (algorithm 1) and the choice $(\mathbf{n}, \boldsymbol{\tau}^k) = (\mathbf{n}_h, \boldsymbol{\tau}_h^k)$ is called the Nitsche method with discrete normals (algorithm 2).

We could have indexed the discrete solutions by the choice of normal, e.g.,

$$\mathbf{u}_h^1 = \mathbf{u}_h^{\mathbf{n}_{\pi}}, \quad p_h^1 = p_h^{\mathbf{n}_{\pi}}, \qquad \mathbf{u}_h^2 = \mathbf{u}_h^{\mathbf{n}_h}, \quad p_h^2 = p_h^{\mathbf{n}_h}.$$

But we chose a more opaque but simpler notation in [5].

Remark 3.1 Polygonal approximations for scalar Dirichlet problems satisfy at best

$$||u - u_h||_{H^1(\Omega_h)} \le Ch^{3/2}$$

for $k \geq 2$ on meshes of size h [2]. The approximation order cannot be higher than 3/2 due to the polygonal approximation of the boundary. Thus there is no compelling reason to choose k > 2 unless the mesh is more refined on Γ than in the interior.

To prove convergence of the polygonal approximations, we need to assume that the solution \mathbf{u} can be extended smoothly to a neighborhood $\widetilde{\Omega}$ of Ω . This guarantees that $\Omega_h \subset \widetilde{\Omega}$ for h sufficiently small.

4 Error estimates

We first write the variational problem in terms of its projection onto the discretely divergencefree subspace, decoupling the pressure from the velocity. Then we review error estimates for the variational crimes arising due to the approximation of the boundary and normal/tangential vectors. Finally, we develop lower bounds for the error in order to identify the most offending terms.

4.1 Problem structure

First define $\Pi_0 = \{q \in \Pi_h^k : \int_{\Omega_h} q \, dx = 0\}$. For $\mathbf{n} \in \{\mathbf{n}_{\pi}, \mathbf{n}_h\}$, define subspaces $Z^{\mathbf{n}}$ of W_h^k by

$$Z^{\mathbf{n}} = \left\{ \mathbf{v} \in W_h^k : \int_{\Omega_h} q \, \nabla \cdot \mathbf{v} \, dx - \oint_{\Gamma_h} q \, (\mathbf{n} \cdot \mathbf{v}) \, ds = 0 \, \forall \, q \in \Pi_0 \right\}.$$
 (22)

In [5], we show that solutions (\mathbf{u}_h^i, p_h^i) defined in (21) satisfy $\mathbf{u}_h^i \in Z^{\mathbf{n}_i}$ and $p_h^i \in \Pi_0$. The equations (21) for \mathbf{u}_h^i then simplify to

$$a(\mathbf{u}_h^i, \mathbf{v}; \mathbf{n}^i) = F(\mathbf{v}) \quad \forall \ \mathbf{v} \in Z^{\mathbf{n}^i}.$$
 (23)

Once \mathbf{u}_h^i is determined, p_h^i can be determined by, $\forall \mathbf{v} \in W_h^k$,

$$b(\mathbf{v}, p_h^i; \mathbf{n}^i) = F(\mathbf{v}) - a(\mathbf{u}_h^i, \mathbf{v}; \mathbf{n}^i), \tag{24}$$

provided that the appropriate inf-sup condition holds [1].

In [5], the following is proved.

Theorem 4.1 The following are equivalent:

- 1. $(\mathbf{u}_h^i, p_h^i, \rho^i)$ is a solution of (21),
- 2. $\mathbf{u}_h^i \in Z^{\mathbf{n}^i}$ is a solution of (23) with $p_h^i \in \Pi_0$ determined by (24).

4.2 Error estimates for $a(\cdot, \cdot; \mathbf{n}_{\pi})$

The first step in [5] is to define appropriate spaces

$$H_N^1(\Omega_h) = \left\{ \mathbf{v} \in H^1(\Omega_h)^d : \mathbf{v} = \mathbf{0} \text{ on } \partial \Omega_h \backslash \Gamma_h, \ \mathcal{D}(\mathbf{v}) \big|_{\Gamma_h} \in L^2(\Gamma_h)^{d^2} \right\}, \tag{25}$$

and

$$\Pi_N(\Omega_h) = \left\{ q \in L^2(\Omega_h) : q \big|_{\Gamma_h} \in L^2(\Gamma_h) \right\}. \tag{26}$$

The form $a(\cdot, \cdot; \mathbf{n})$ is coercive and continuous in $H_N^1(\Omega_h)$ for both choices of normal and tangent vectors, for γ sufficiently large. The proof of this is standard [11]. This is why the solution \mathbf{u}_h^i of (21) is uniquely determined for γ sufficiently large. On $H_N^1(\Omega_h)$, define the norms

$$\| \mathbf{v} \|_{\pi} = \left(a(\mathbf{v}, \mathbf{v}; \mathbf{n}_{\pi}) \right)^{1/2}, \qquad \| \mathbf{v} \|_{h} = \left(a(\mathbf{v}, \mathbf{v}; \mathbf{n}_{h}) \right)^{1/2}$$
 (27)

for all $\mathbf{v} \in H_N^1(\Omega_h)$.

It is assumed in [5] that the mesh is nondegenerate [1], so that the ratio of mesh sizes in neighboring elements is uniformly bounded, and that the mesh-size function h that appears in the penalty terms in the bilinear forms is piecewise constant on elements. For boundary edges or faces $e \in \Gamma_h$, h_e denotes this constant value in the corresponding triangle or simplex, h_{Γ} denotes the maximum value of h_e for all $e \subset \Gamma_h$, and h_{Ω} denote the maximum mesh size for all elements in the mesh for Ω_h .

The analog of Lemma 3.1 does not hold exactly for the polygonal approximation. First, we need to assume that \mathbf{u} and p have been extended outside of Ω to be in $H_N^1(\Omega_h) \times \Pi$. In particular, we assume that \mathbf{u} and p have been extended to a domain $\widetilde{\Omega}$ that contains Ω_h for h_{Γ} sufficiently small. We also assume that the finite element functions are similarly extended outside of Ω_h as polynomials locally.

To begin with, we assume that our solution satisfies (1) in a slightly larger domain $\widetilde{\Omega}$, so that we can integrate by parts on Ω_h [5] to get

$$\frac{\nu}{2}(\mathcal{D}(\mathbf{u}), \mathcal{D}(\mathbf{v}))_h + (\mathbf{u} \cdot \nabla \mathbf{u}, \mathbf{v})_h - (p, \nabla \cdot \mathbf{v})_h = \oint_{\Gamma_h} \mathbf{n}_h^t (\nu \mathcal{D}(\mathbf{u}) - pI) \mathbf{v} \, ds$$
 (28)

for all $\mathbf{v} \in H^1(\widetilde{\Omega})^d$. This holds for potential flow due to the formulas in section 2. The following is proved in [5, Lemma 3.3].

Lemma 4.1 Let (\mathbf{u}, p) be the solution of (1) in $H^1(\widetilde{\Omega})^d$, satisfying the boundary conditions (2) and (3). Suppose that $\mathbf{v} \in W_h^k$. Then

$$a(\mathbf{u}, \mathbf{v}; \mathbf{n}_{\pi}) + (\mathbf{u} \cdot \nabla \mathbf{u}, \mathbf{v})_{h} - (p, \nabla \cdot \mathbf{v})_{h} + \oint_{\Gamma_{h}} p \, \mathbf{n}_{h} \cdot \mathbf{v} \, ds$$

$$= \oint_{\Gamma_{h}} \left(\beta(\mathbf{u} - \mathbf{u} \circ \boldsymbol{\pi}) + \nu \, \mathbf{n}_{\pi}^{t} \left(\mathcal{D}(\mathbf{u}) - \mathcal{D}(\mathbf{u}) \circ \boldsymbol{\pi} \right) \right) \cdot P_{\tau} \mathbf{v} \, ds - \oint_{\Gamma_{h}} \nu \left(\mathbf{n}_{\pi} - \mathbf{n}_{h} \right)^{t} \mathcal{D}(\mathbf{u}) \mathbf{v} \, ds \quad (29)$$

$$- \oint_{\Gamma_{h}} \nu \, \mathbf{n}_{\pi}^{t} \mathcal{D}(\mathbf{v}) \mathbf{n}_{\pi} (\mathbf{n}_{\pi} \cdot (\mathbf{u} - \mathbf{u} \circ \boldsymbol{\pi})) \, ds + \gamma \oint_{\Gamma_{h}} h^{-1} ((\mathbf{u} - \mathbf{u} \circ \boldsymbol{\pi}) \cdot \mathbf{n}_{\pi}) (\mathbf{v} \cdot \mathbf{n}_{\pi}) \, ds.$$

4.3 Estimating terms in Lemma 4.1

We use standard inverse estimates [1, section 4.5], namely

$$\|\mathbf{v}\|_{W_{\infty}^{l}(e)} \le Ch_e^{1-d/2-l}\|\mathbf{v}\|_{H^1(T_e)}, \quad l = 0, 1, 2,$$
 (30)

where $W_{\infty}^0 = L^{\infty}$ and d is the dimension of Ω . Thus it is proved in [5, (3.18)] that

$$\left| \oint_{\Gamma_h} (\mathbf{n}_h - \mathbf{n}_\pi)^t \mathcal{D}(\mathbf{u}) \mathbf{v} \, ds \right| \le C h_\Gamma^{3/2} \| \mathbf{u} \|_{W_\infty^1(\widetilde{\Omega})} \| \mathbf{v} \|_{H^1(\Omega_h)}, \tag{31}$$

where $h_{\Gamma} = \max_{e \in \Gamma_h} h_e$. This uses the estimate

$$\sqrt{\sum_{e \in \Gamma_h} \left(h_e^{1+d/2}\right)^2} \le C h_{\Gamma}^{3/2}. \tag{32}$$

To estimate the remaining terms in (29), observe that we can write (in two dimensions) each edge e as

$$e = \{(x,0) \ : \ 0 \le x \le h\}$$

by choosing suitable coordinates. In these coordinates,

$$\mathbf{u} \circ \boldsymbol{\pi}(x,0) = \mathbf{u}(x,\delta(x)), \quad 0 \le x \le h, \tag{33}$$

where δ is of order h^2 , since it represents the error in a linear approximation of Γ . A similar representation holds in three dimensions. Note that $1/C \leq h/h_e \leq C$ since the mesh is nondegenerate. Thus Taylor's theorem implies

$$\|\mathbf{u} - \mathbf{u} \circ \boldsymbol{\pi}\|_{L^{\infty}(e)} \le Ch_e^2 \|\mathbf{u}\|_{W_{-\infty}^1(\widetilde{\Omega})}, \quad \|\mathcal{D}(\mathbf{u}) - \mathcal{D}(\mathbf{u}) \circ \boldsymbol{\pi}\|_{L^{\infty}(e)} \le Ch_e^2 \|\mathbf{u}\|_{W_{-\infty}^2(\widetilde{\Omega})}$$

for all $e \in \Gamma_h$. Thus it is proved in [5, (3.21-23)] that

$$\left| \oint_{\Gamma_h} \mathbf{n}_{\pi}^t \mathcal{D}(\mathbf{v}) \mathbf{n}_{\pi} (\mathbf{n}_{\pi} \cdot (\mathbf{u} - \mathbf{u} \circ \boldsymbol{\pi})) \, ds \right| \le C h_{\Gamma}^{3/2} \|\mathbf{u}\|_{W_{\infty}^1(\widetilde{\Omega})} \|\mathbf{v}\|_{H^1(\Omega_h)}, \tag{34}$$

$$\left| \oint_{\Gamma_h} h^{-1}((\mathbf{u} - \mathbf{u} \circ \boldsymbol{\pi}) \cdot \mathbf{n}_{\pi})(\mathbf{v} \cdot \mathbf{n}_{\pi}) ds \right| \le C h_{\Gamma}^{3/2} \|\mathbf{u}\|_{W_{\infty}^{1}(\widetilde{\Omega})} \left(\oint_{\Gamma_h} h^{-1} |\mathbf{v} \cdot \mathbf{n}_{\pi}|^2 ds \right)^{1/2}, \quad (35)$$

and

$$\left| \oint_{\Gamma_h} \left(\beta(\mathbf{u} - \mathbf{u} \circ \boldsymbol{\pi}) + \nu \, \mathbf{n}_{\pi}^t \left(\mathcal{D}(\mathbf{u}) - \mathcal{D}(\mathbf{u}) \circ \boldsymbol{\pi} \right) \cdot P_{\tau} \mathbf{v} \, ds \right| \leq C h_{\Gamma}^{5/2} \|\mathbf{u}\|_{W_{\infty}^2(\widetilde{\Omega})} \|\mathbf{v}\|_{H^1(\Omega_h)}. \tag{36}$$

Combining (31), (34), (35), and (36), Lemma 4.1 implies the following:

Lemma 4.2 Let (\mathbf{u}, p) be the solution of (1) and assume that the mesh is nondegenerate. Suppose that $\mathbf{v}_h \in W_h^k$. Then

$$\left| a(\mathbf{u}, \mathbf{v}_{h}; \mathbf{n}_{\pi}) + (\mathbf{u} \cdot \nabla \mathbf{u}, \mathbf{v}_{h})_{h} - (p, \nabla \cdot \mathbf{v}_{h})_{h} + \oint_{\Gamma_{h}} p \, \mathbf{v}_{h} \cdot \mathbf{n}_{h} \, ds \right|$$

$$\leq C \sum_{\ell=0}^{1} h_{\Gamma}^{3/2+\ell} \|\mathbf{u}\|_{W_{\infty}^{1+\ell}(\widetilde{\Omega})} \|\mathbf{v}_{h}\|_{\pi},$$
(37)

where C depends only on the shape regularity of the mesh, ν , β , and γ , and h_{Γ} is the maximum mesh size near Γ .

Suppose that

$$a(\mathbf{u}_h, \mathbf{v}_h; \mathbf{n}_{\pi}) + (\mathbf{u}_h \cdot \nabla \mathbf{u}_h, \mathbf{v}_h)_h = 0$$
(38)

for all $\mathbf{v}_h \in Z^{\mathbf{n}_{\pi}}$. Then the following is proved in [5, 3.30]:

$$\frac{1}{2} \| \mathbf{u} - \mathbf{u}_h \|_{\pi}^2 \leq \frac{5}{4} \| \mathbf{u} - \mathbf{v}_h \|_{\pi}^2 + 2 \left(C h_{\Gamma}^{3/2} \| \mathbf{u} \|_{W_{\infty}^2(\widetilde{\Omega})} \right)^2
+ C \left(\| p - q \|_{L^2(\Omega_h)} + \| p - q \|_{L^r(\Gamma_h)} \right) \| \mathbf{v}_h - \mathbf{u}_h \|_{H^1(\Omega_h)}
+ \left(\mathbf{u}_h \cdot \nabla \mathbf{u}_h - \mathbf{u} \cdot \nabla \mathbf{u}, \mathbf{v}_h - \mathbf{u}_h \right)_h,$$
(39)

where r = 1 for d = 2 and r = 4/3 for d = 3.

4.3.1 Estimating the nonlinear term

The following proof was not included in [5] due to limitations of space and the fact that the arguments are standard. We have for any $\mathbf{w} \in W_h^k$

$$|(\mathbf{u}_{h} \cdot \nabla \mathbf{u}_{h} - \mathbf{u} \cdot \nabla \mathbf{u}, \mathbf{w})_{h}| \leq |((\mathbf{u}_{h} - \mathbf{u}) \cdot \nabla \mathbf{u}_{h}, \mathbf{w})_{h}| + |(\mathbf{u} \cdot \nabla (\mathbf{u}_{h} - \mathbf{u}), \mathbf{w})_{h}|$$

$$\leq ||\mathbf{u}_{h} - \mathbf{u}||_{H^{1}(\Omega_{h})} (||\mathbf{u}_{h}||_{H^{1}(\Omega_{h})} + ||\mathbf{u}||_{H^{1}(\Omega_{h})}) ||\mathbf{w}||_{H^{1}(\Omega_{h})}$$
(40)

since Cauchy–Schwarz and Sobolev's inequality [1, 3] imply

$$\begin{aligned} |(\mathbf{u} \cdot \nabla \mathbf{v}, \mathbf{w})_h| &\leq C \|\mathbf{v}\|_{H^1(\Omega_h)} \||\mathbf{u}| \|\mathbf{w}|\|_{L^2(\Omega_h)} \leq C \|\mathbf{v}\|_{H^1(\Omega_h)} \|\mathbf{u}\|_{L^4(\Omega_h)} \|\mathbf{w}\|_{L^4(\Omega_h)} \\ &\leq C \|\mathbf{v}\|_{H^1(\Omega_h)} \|\mathbf{u}\|_{H^1(\Omega_h)} \|\mathbf{w}\|_{H^1(\Omega_h)}. \end{aligned}$$

Combining (39) and (40), we get

$$\frac{1}{2} \| \mathbf{u} - \mathbf{u}_h \|_{\pi}^2 \leq \frac{5}{4} \| \mathbf{u} - \mathbf{v}_h \|_{\pi}^2 + 2 \left(C h_{\Gamma}^{3/2} \| \mathbf{u} \|_{W_{\infty}^2(\widetilde{\Omega})} \right)^2
+ C \left(\| p - q \|_{L^2(\Omega_h)} + \| p - q \|_{L^r(\Gamma_h)}
+ \| \mathbf{u}_h - \mathbf{u} \|_{H^1(\Omega_h)} \left(\| \mathbf{u}_h \|_{H^1(\Omega_h)} + \| \mathbf{u} \|_{H^1(\Omega_h)} \right) \right) \| \mathbf{v}_h - \mathbf{u}_h \|_{H^1(\Omega_h)}.$$
(41)

Let us denote two quantities as follows:

$$E_p = \inf_{q \in \Pi_0} (\|p - q\|_{L^2(\Omega_h)} + \|p - q\|_{L^r(\Gamma_h)}), \quad B = \|\mathbf{u}_h\|_{H^1(\Omega_h)} + \|\mathbf{u}\|_{H^1(\Omega_h)}.$$

Taking the infimum over $q \in \Pi_0$ in (41), using the triangle inequality, and applying the arithmetic-geometric mean inequality a few times yields

$$\frac{1}{2} \| \mathbf{u} - \mathbf{u}_{h} \|_{\pi}^{2} \leq \frac{5}{4} \| \mathbf{u} - \mathbf{v}_{h} \|_{\pi}^{2} + 2 \left(C h_{\Gamma}^{3/2} \| \mathbf{u} \|_{W_{\infty}^{2}(\widetilde{\Omega})} \right)^{2} \\
+ C \left(E_{p} + B \| \mathbf{u}_{h} - \mathbf{u} \|_{H^{1}(\Omega_{h})} \right) \| \mathbf{v}_{h} - \mathbf{u}_{h} \|_{H^{1}(\Omega_{h})} \\
\leq \frac{5}{4} \| \mathbf{u} - \mathbf{v}_{h} \|_{\pi}^{2} + 2 \left(C h_{\Gamma}^{3/2} \| \mathbf{u} \|_{W_{\infty}^{2}(\widetilde{\Omega})} \right)^{2} + \\
C \left(E_{p} + B \| \mathbf{u}_{h} - \mathbf{u} \|_{H^{1}(\Omega_{h})} \right) \left(\| \mathbf{v}_{h} - \mathbf{u} \|_{H^{1}(\Omega_{h})} + \| \mathbf{u} - \mathbf{u}_{h} \|_{H^{1}(\Omega_{h})} \right) \\
\leq \frac{5}{4} \| \mathbf{u} - \mathbf{v}_{h} \|_{\pi}^{2} + 2 \left(C h_{\Gamma}^{3/2} \| \mathbf{u} \|_{W_{\infty}^{2}(\widetilde{\Omega})} \right)^{2} \\
+ C B \| \mathbf{u} - \mathbf{u}_{h} \|_{H^{1}(\Omega_{h})}^{2} + C E_{p} \| \mathbf{u}_{h} - \mathbf{u} \|_{H^{1}(\Omega_{h})} \\
+ C \left(E_{p} + B \| \mathbf{u}_{h} - \mathbf{u} \|_{H^{1}(\Omega_{h})} \right) \| \mathbf{v}_{h} - \mathbf{u} \|_{H^{1}(\Omega_{h})} \\
\leq \frac{5}{4} \| \mathbf{u} - \mathbf{v}_{h} \|_{\pi}^{2} + 2 \left(C h_{\Gamma}^{3/2} \| \mathbf{u} \|_{W_{\infty}^{2}(\widetilde{\Omega})} \right)^{2} + 2 C B \| \mathbf{u} - \mathbf{u}_{h} \|_{H^{1}(\Omega_{h})}^{2} \\
+ 2 \left(C E_{p} \right)^{2} + \frac{1}{4} \| \mathbf{u}_{h} - \mathbf{u} \|_{H^{1}(\Omega_{h})}^{2} + \left(\frac{1}{4} + C B \right) \| \mathbf{v}_{h} - \mathbf{u} \|_{H^{1}(\Omega_{h})}^{2} \\
= \left(\frac{3}{2} + C B \right) \| \mathbf{u} - \mathbf{v}_{h} \|_{\pi}^{2} + 2 \left(C h_{\Gamma}^{3/2} \| \mathbf{u} \|_{W_{\infty}^{2}(\widetilde{\Omega})} \right)^{2} \\
+ \left(\frac{1}{4} + 2 C B \right) \| \mathbf{u} - \mathbf{u}_{h} \|_{H^{1}(\Omega_{h})}^{2} + 2 \left(C E_{p} \right)^{2}.$$

Due to the coercivity of $a(\cdot, \cdot; \mathbf{n}_{\pi})$, standard techniques [3] show that both \mathbf{u} and \mathbf{u}_h are small when the boundary data \mathbf{g} is small with respect to ν , and so B is small. This leads to the following.

Theorem 4.2 Let \mathbf{u}_h and p_h be defined by (21). Suppose that $\nu^{-1}\mathbf{g}$ is sufficiently small and that the mesh is nondegenerate. Let (\mathbf{u}, p) be the unique solution of (1), and let (\mathbf{u}_h^1, p_h^1) be the unique solution of (21) with $F(\mathbf{v}) = -(\mathbf{u}_h^1 \cdot \nabla \mathbf{u}_h^1, \mathbf{v})_h$. Suppose that $\mathbf{u}_h \in Z$ solves (38). Then

$$\| \mathbf{u} - \mathbf{u}_h \|_{\pi} \le C h_{\Gamma}^{3/2} (\| \mathbf{u} \|_{W_{\infty}^2(\widetilde{\Omega})} + \| p \|_{W_{\infty}^1(\widetilde{\Omega})}) + C \Big(\inf_{\mathbf{v}_h \in Z} \| \mathbf{u} - \mathbf{v}_h \|_{H^1(\Omega_h)} + \inf_{q \in \Pi_0} (\| p - q \|_{L^2(\Omega_h)} + \| p - q \|_{L^r(\partial \Omega_h)}) \Big),$$
(43)

where r = 1 for d = 2 and r = 4/3 for d = 3 and C depends only on the shape regularity of the mesh, β , ν , and γ , and h_{Γ} is the maximum mesh size near Γ .

Using the inf-sup condition [1] for the pair W_h^k and Π_h^k , the following is proved in [5].

Theorem 4.3 Let \mathbf{u}_h and p_h be defined by (21). Suppose that $\nu^{-1}\mathbf{g}$ is sufficiently small and that the mesh is nondegenerate. Let (\mathbf{u}, p) be the solution of (1). Then

$$\| \mathbf{u} - \mathbf{u}_h \|_{\pi} + \| p - p_h \|_{L^2(\Omega_h)} \le C h_{\Gamma}^{3/2} (\| \mathbf{u} \|_{W_{\infty}^2(\widetilde{\Omega})} + \| p \|_{W_{\infty}^1(\widetilde{\Omega})}) + C h_{\Omega}^k (\| \mathbf{u} \|_{H^{k+1}(\Omega_h)} + \| p \|_{H^k(\Omega_h)} + \| p \|_{W_r^k(\partial \Omega_h)}),$$

$$(44)$$

h_{Ω}	0.001	0.01	0.1	1.0	10.0	100
0.591	0.9518	0.9521	0.9554	0.9657	0.8388	1.4673
0.328	0.3013	0.3014	0.3023	0.3086	0.3278	0.5802
0.165	0.0885	0.1687	0.0872	0.0899	0.1050	0.2042
0.086	0.0215	0.0215	0.0216	0.0227	0.0306	0.0666
nco	2.0	2.0	2.0	1.9	1.7	1.6

Table 1: Approach 1: Nitsche method with projected normal. Error and averaged numerically computed convergence order (nco) measured in the $\|\|\mathbf{u}\|\|_1 + \|p\|_{L^2}$ -norm for uniform meshes of mesh size h_{Ω} , using k = 2, \mathbf{n}_{π} for the normal and $\boldsymbol{\tau}_{\pi}$ for tangent, for different values of γ .

where r=1 for d=2 and r=4/3 for d=3 and C depends only on the shape regularity of the mesh, β , ν , and γ , h_{Γ} is the maximum mesh size near Γ , and h_{Ω} is the maximum mesh over all of Ω .

Figure 1 shows the results of a computation using the first algorithm on a coarse mesh. Table 1 gives numerical confirmation of the error estimates.

Table 1 indicates a feature of Nitsche's method with regard to the choice of penalty parameter γ [8, section 22.4]. For certain values of γ and h, the errors can suddenly increase significantly. The offending error value is highlighted in bold in Table 1, the error for $h_{\Omega} = 0.165$ and $\gamma = 0.01$. For other values of γ for the same value of h_{Ω} , the errors are significantly smaller, and for the same value of γ and different values of h_{Ω} , the errors are as expected. Otherwise, the parameter γ has little effect on the errors for $\gamma \leq 1$. However, for $\gamma \geq 10$, there is a slight degradation.

Table 2 confirms the implication of Theorem 4.3 that the error will not decrease substantially as k is increased, unless the mesh is substantially refined near Γ .

4.4 Estimates for $a(\cdot, \cdot; \mathbf{n}_h)$

Analogous to Lemma 4.1, it is proved in [5] that

$$a(\mathbf{u}, \mathbf{v}; \mathbf{n}_{h}) + (\mathbf{u} \cdot \nabla \mathbf{u}, \mathbf{v})_{h} - (p, \nabla \cdot \mathbf{v})_{h} + \oint_{\Gamma_{h}} p \, \mathbf{n}_{h}^{t} \mathbf{v} \, ds$$

$$= \oint_{\Gamma_{h}} \nu \left(\mathbf{n}_{h}^{t} \mathcal{D}(\mathbf{u}) - \mathbf{n}_{\pi}^{t} \left(\mathcal{D}(\mathbf{u}) \circ \boldsymbol{\pi} \right) \right) \mathbf{v} \, ds$$

$$+ \oint_{\Gamma_{h}} \sum_{i} \beta \left((\mathbf{u} \cdot \boldsymbol{\tau}_{h}^{i}) (\mathbf{v} \cdot \boldsymbol{\tau}_{h}^{i}) - (\mathbf{u} \circ \boldsymbol{\pi} \cdot \boldsymbol{\tau}_{\pi}^{i}) (\mathbf{v} \cdot \boldsymbol{\tau}_{\pi}^{i}) \right) ds$$

$$+ \oint_{\Gamma_{h}} \mathbf{n}_{\pi}^{t} \left((\nu \mathcal{D}(\mathbf{u})) \circ \boldsymbol{\pi} \right) \mathbf{n}_{\pi} (\mathbf{n}_{\pi} \cdot \mathbf{v}) \, ds - \oint_{\Gamma_{h}} \mathbf{n}_{h}^{t} \left(\nu \mathcal{D}(\mathbf{u}) \right) \mathbf{n}_{h} (\mathbf{n}_{h} \cdot \mathbf{v}) \, ds$$

$$- \oint_{\Gamma_{h}} \mathbf{n}_{h}^{t} \left(\nu \mathcal{D}(\mathbf{v}) \right) \mathbf{n}_{h} (\mathbf{n}_{h} \cdot \mathbf{u}) \, ds + \gamma \oint_{\Gamma_{h}} h^{-1} (\mathbf{u} \cdot \mathbf{n}_{h}) (\mathbf{v} \cdot \mathbf{n}_{h}) \, ds.$$

$$(45)$$

h_{Ω}	2	3	4
0.591	0.8388	0.8625	0.8205
0.328	0.3278	0.3222	0.2951
0.165	0.1051	0.1109	0.1075
nco	1.6	1.6	1.6

Table 2: (Approach 1) Error measured in the $\|\|\mathbf{u}\|\|_1 + \|p\|_{L^2}$ -norm for $\gamma = 10$ on uniform meshes of mesh size h_{Ω} , for different values of k using \mathbf{n}_{π} for the normal and $\boldsymbol{\tau}_{\pi}$ for tangent.

Each of these terms is then estimated in [5].

For the first term in (45),

$$\left| \oint_{\Gamma_h} \left(\mathbf{n}_h^t \mathcal{D}(\mathbf{u}) - \mathbf{n}_\pi^t \left(\mathcal{D}(\mathbf{u}) \circ \boldsymbol{\pi} \right) \right) \mathbf{v} \, ds \right| \le C \|\mathbf{u}\|_{W_{\infty}^1(\widetilde{\Omega})} \sum_{e \in \Gamma_h} h_e^{1 + d/2} \|\mathbf{v}\|_{H^1(T_e)}, \tag{46}$$

using the inverse estimate (30). Therefore (32) implies

$$\left| \oint_{\Gamma_h} \left(\mathbf{n}_h^t \mathcal{D}(\mathbf{u}) - \mathbf{n}_\pi^t \left(\mathcal{D}(\mathbf{u}) \circ \boldsymbol{\pi} \right) \right) \mathbf{v} \, ds \right| \le C h_{\Gamma}^{3/2} \|\mathbf{u}\|_{W_{\infty}^1(\widetilde{\Omega})} \|\mathbf{v}\|_{H^1(\Omega_h)}. \tag{47}$$

For the next term in (45),

$$\left| \oint_{\Gamma_h} (\mathbf{u} \cdot \boldsymbol{\tau}_h^i) (\mathbf{v} \cdot \boldsymbol{\tau}_h^i) - (\mathbf{u} \circ \boldsymbol{\pi} \cdot \boldsymbol{\tau}_\pi^i) (\mathbf{v} \cdot \boldsymbol{\tau}_\pi^i) \, ds \right| \le C h_{\Gamma}^{3/2} \|\mathbf{u}\|_{W_{\infty}^1(\widetilde{\Omega})} \|\mathbf{v}\|_{H^1(\Omega_h)}, \tag{48}$$

using (30) and (32).

Similarly, adding and subtracting $\mathbf{n}_h^t \mathcal{D}(\mathbf{u}) \mathbf{n}_h(\mathbf{n}_{\pi} \cdot \mathbf{v})$ gives

$$\left| \oint_{\Gamma_h} \mathbf{n}_{\pi}^t (\mathcal{D}(\mathbf{u}) \circ \boldsymbol{\pi}) \mathbf{n}_{\pi} (\mathbf{n}_{\pi} \cdot \mathbf{v}) - \mathbf{n}_h^t \mathcal{D}(\mathbf{u}) \mathbf{n}_h (\mathbf{n}_h \cdot \mathbf{v}) \, ds \right| \le C h_{\Gamma}^{3/2} \|\mathbf{u}\|_{W_{\infty}^2(\widetilde{\Omega})} \|\mathbf{v}\|_{H^1(\Omega_h)}, \quad (49)$$

using (30) and (32) as in (48). Collecting what we have proved so far, we have

$$\left| a(\mathbf{u}, \mathbf{v}; \mathbf{n}_{h}) + (\mathbf{u} \cdot \nabla \mathbf{u}, \mathbf{v})_{h} - (p, \nabla \cdot \mathbf{v})_{h} + \oint_{\Gamma_{h}} p \, \mathbf{n}_{h}^{t} \mathbf{v} \, ds \right|
+ \oint_{\Gamma_{h}} \mathbf{n}_{h}^{t} (\nu \mathcal{D}(\mathbf{v})) \mathbf{n}_{h} (\mathbf{n}_{h} \cdot \mathbf{u}) \, ds - \gamma \oint_{\Gamma_{h}} h^{-1} (\mathbf{u} \cdot \mathbf{n}_{h}) (\mathbf{v} \cdot \mathbf{n}_{h}) \, ds \right|
\leq C h_{\Gamma}^{3/2} \|\mathbf{u}\|_{W_{-1}^{1}(\widetilde{\Omega})} \|\mathbf{v}\|_{H^{1}(\Omega_{h})}.$$
(50)

The remaining two terms in (45) now appear as the middle line in (50).

Since $\mathbf{n}_{\pi} \cdot (\mathbf{u} \circ \boldsymbol{\pi}) \equiv 0$ on Γ_h , on each e,

$$|\mathbf{n}_{h} \cdot \mathbf{u}| = |\mathbf{n}_{h} \cdot \mathbf{u} - \mathbf{n}_{\pi} \cdot (\mathbf{u} \circ \boldsymbol{\pi})| = |(\mathbf{n}_{h} - \mathbf{n}_{\pi}) \cdot \mathbf{u}| + |\mathbf{n}_{\pi} \cdot (\mathbf{u} - \mathbf{u} \circ \boldsymbol{\pi})|$$

$$\leq C \sum_{\ell=0}^{1} h_{e}^{\ell+1} ||\mathbf{u}||_{W_{\infty}^{\ell}(\widetilde{\Omega})} \leq C h_{e} ||\mathbf{u}||_{W_{\infty}^{1}(\widetilde{\Omega})}.$$
(51)

Thus

$$\left| \oint_{\Gamma_h} \mathbf{n}_h^t \mathcal{D}(\mathbf{v}) \mathbf{n}_h(\mathbf{n}_h \cdot \mathbf{u}) \, ds \right| \le C h_{\Gamma}^{1/2} \|\mathbf{u}\|_{W_{\infty}^1(\widetilde{\Omega})} \|\mathbf{v}\|_{H^1(\Omega_h)}, \tag{52}$$

using (30) and (32). Finally, (51) implies that

$$\left| \oint_{\Gamma_{t}} h^{-1}(\mathbf{n}_{h} \cdot \mathbf{u})(\mathbf{v} \cdot \mathbf{n}_{h}) ds \right| \leq C h_{\Gamma}^{1/2} \|\mathbf{u}\|_{W_{\infty}^{1}(\widetilde{\Omega})} \|\mathbf{v}\|_{h}.$$
 (53)

Thus we see that the two terms on the last line of (45) are bigger by a factor of h_{Γ}^{-1} than the other terms in (45). Therefore, the analog of Theorem 4.2 has an error of only $h_{\Gamma}^{1/2}$.

Theorem 4.4 Suppose that \mathbf{g} is sufficiently small and that the mesh is nondegenerate. Let (\mathbf{u}, p) be the unique solution of (1), and let (\mathbf{u}_h^2, p_h^2) be the unique solution of (21) with $F(\mathbf{v}) = -(\mathbf{u}_h^2 \cdot \nabla \mathbf{u}_h^2, \mathbf{v})_h$. Suppose that $\mathbf{u}_h \in Z$ solves (38). Then

$$\|\|\mathbf{u} - \mathbf{u}_{h}^{2}\|\|_{h} \le C \sum_{\ell=0}^{1} h_{\Gamma}^{\ell+1/2} \|\mathbf{u}\|_{W_{\infty}^{1+\ell}(\widetilde{\Omega})} + C \left(\inf_{\mathbf{v} \in Z} \|\mathbf{u} - \mathbf{v}\|_{H^{1}(\Omega_{h})} + \inf_{q \in \Pi_{0}} \|p - q\|_{L^{2}(\Omega_{h})}\right), \quad (54)$$

where C depends only on the shape regularity of the mesh, β , ν , and γ , and h_{Γ} is the maximum mesh size near Γ .

Using the inf-sup condition for the pair W_h^k and Π_h^k , we conclude the following [1].

Theorem 4.5 Suppose that \mathbf{g} is sufficiently small and that the mesh is nondegenerate. Let (\mathbf{u}, p) be the solution of (1). Then

$$\|\|\mathbf{u} - \mathbf{u}_h^2\|\|_h + \|p - p_h^2\|_{L^2(\Omega_h)} \le C \sum_{\ell=0}^1 h_{\Gamma}^{\ell+1/2} \|\mathbf{u}\|_{W_{\infty}^{1+\ell}(\widetilde{\Omega})} + C h_{\Omega}^k (\|\mathbf{u}\|_{H^{k+1}(\Omega_h)} + \|p\|_{H^k(\Omega_h)}), (55)$$

where C depends only on the shape regularity of the mesh, β , ν , and γ , h_{Γ} is the maximum mesh size near Γ , and h_{Ω} is the maximum mesh over all of Ω .

Thus the error for method 2 appears to be worse than for method 1 by a factor of h_{Γ}^{-1} , as is found computationally for the potential-flow problem, documented in Table 3.

5 Lower bounds for the error

As is well known [10], when there is a variational crime, it is possible to give lower bounds for the resulting error. This is based on the Cauchy–Schwarz inequality

$$a(\mathbf{u} - \mathbf{u}_h^i, \mathbf{v}; \mathbf{n}_i) \le \| \|\mathbf{u} - \mathbf{u}_h^i \|_i \| \|\mathbf{v} \|_i, \quad i \in \{\pi, h\},$$

$$(56)$$

for any \mathbf{v} . Dividing by the norm of \mathbf{v} , we find

$$\|\|\mathbf{u} - \mathbf{u}_h^i\|\|_i \ge \frac{a(\mathbf{u} - \mathbf{u}_h^i, \mathbf{v}; \mathbf{n})}{\|\|\mathbf{v}\|\|_i}, \ i = 1, 2,$$
(57)

h_{Ω}	0.001	0.01	0.1	1.0	10.0	100.0
0.591	1.6561	1.6531	1.6232	1.3809	2.8539	14.9036
0.328	1.1042	1.1541	1.1362	1.1449	2.2288	12.6495
0.165	0.7333	0.7322	0.7218	0.8644	1.3568	8.7213
0.086	0.4463	0.4458	0.4538	0.4118	0.8030	5.3767
nco	0.7	0.7	0.7	0.6	0.6	0.5

Table 3: Approach 2: Nitsche method with discrete normal. Error and convergence rates measured in the $\|\mathbf{u}\|_h + \|p\|_{L^2}$ -norm for uniform meshes of mesh size h_{Ω} , using k = 2, \mathbf{n}_h for the normal, $\boldsymbol{\tau}_h$ for tangent, and different values of γ .

h_{Ω}	1	2	3
0.591	2.8539	2.9385	4.7645
0.328	2.2288	2.5597	3.5556
0.165	1.3568	1.7826	2.3600
0.086	0.8030	1.3647	1.8863
nco	0.6	0.6	0.5

Table 4: (Nitsche method with discrete normal) Error measured in the $\|\|\mathbf{u}\|\|_h + \|p\|_{L^2}$ -norm for uniform meshes of mesh size h_{Ω} with $\gamma = 10$ and different values of k.

for any \mathbf{v} . Now let us specialize to the second algorithm with discrete normals and tangents. From (50), we have for $\mathbf{v} \in \mathbb{Z}$

$$\left| a(\mathbf{u} - \mathbf{u}_{h}^{2}, \mathbf{v}; \mathbf{n}_{h}) + \oint_{\Gamma_{h}} \mathbf{n}_{h}^{t} \left(\frac{\gamma}{h} \mathbf{v} - \nu \mathcal{D}(\mathbf{v}) \mathbf{n}_{h} \right) (\mathbf{u} \cdot \mathbf{n}_{h}) ds \right|$$

$$\leq C h_{\Gamma}^{3/2} \|\mathbf{u}\|_{W_{\infty}^{2}(\widetilde{\Omega})} + C h_{\Omega}^{k} (\|\mathbf{u}\|_{H^{k+1}(\Omega_{h})} + \|p\|_{H^{k}(\Omega_{h})}).$$

$$(58)$$

Now we choose [9] a special $\mathbf{v} \in Z$ so that

$$\|\mathbf{u} - \mathbf{v}\|_{H^1(\Omega_h)} \le Ch_{\Omega}^k \|\mathbf{u}\|_{H^{k+1}(\Omega_h)}, \quad \|\mathbf{u} - \mathbf{v}\|_{L^1(\Gamma_h)} \le Ch_{\Gamma}^{k+1} \|\mathbf{u}\|_{W_1^{k+1}(\Gamma_h)},$$
 (59)

valid for k = 2. Note that \mathbf{v} is not constrained by any boundary conditions on Γ_h . Since the approximation operator defined in [9] is local, it is easy to see that the constant C is independent of h even though the domain changes with h.

Let \mathbf{u}_I be the interpolant of \mathbf{u} in W_h^k . Then

$$\|\mathcal{D}(\mathbf{u}) - \mathcal{D}(\mathbf{v})\|_{L^{1}(\Gamma_{h})} \leq \|\mathcal{D}(\mathbf{u}) - \mathcal{D}(\mathbf{u}_{I})\|_{L^{1}(\Gamma_{h})} + \|\mathcal{D}(\mathbf{u}_{I}) - \mathcal{D}(\mathbf{v})\|_{L^{1}(\Gamma_{h})}$$

$$\leq Ch_{\Gamma}^{k} \|\mathcal{D}(\mathbf{u})\|_{W_{1}^{k+1}(\Gamma_{h})} + Ch_{\Gamma}^{1-d/2} \|\mathbf{u}_{I} - \mathbf{v}\|_{H^{1}(\Omega_{h})}$$

$$\leq Ch_{\Gamma}^{k} \|\mathcal{D}(\mathbf{u})\|_{W_{1}^{k+1}(\Gamma_{h})} + Ch_{\Gamma}^{1-d/2} h_{\Omega}^{k} \|\mathbf{u}\|_{H^{k+1}(\Omega_{h})}.$$

$$(60)$$

We now re-examine (52) for this **v**. Since $\mathbf{n}_h \cdot \mathbf{u} = \mathcal{O}(h_{\Gamma})$ on Γ_h , (60) implies

$$\left| \oint_{\Gamma_h} \mathbf{n}_h^t (\nu \mathcal{D}(\mathbf{v})) \mathbf{n}_h(\mathbf{n}_h \cdot \mathbf{u}) \, ds \right| \leq \left| \oint_{\Gamma_h} \mathbf{n}_h^t (\nu \mathcal{D}(\mathbf{u})) \mathbf{n}_h(\mathbf{n}_h \cdot \mathbf{u}) \, ds \right|$$

$$+ C \left(h_{\Gamma}^k \| \mathcal{D}(\mathbf{u}) \|_{W_1^{k+1}(\Gamma_h)} + h_{\Gamma}^{1-d/2} h_{\Omega}^k \| \mathbf{u} \|_{H^{k+1}(\Omega_h)} \right) \| \mathbf{u} \|_{L^{\infty}(\Gamma_h)} \leq C h_{\Gamma}^{3/2},$$
(61)

provided $h_{\Omega}^k \leq C h_{\Gamma}^{(1+d)/2}$ and **u** is sufficiently smooth. Therefore, (58) implies

$$\left| a(\mathbf{u} - \mathbf{u}_h^2, \mathbf{v}; \mathbf{n}_h) + \gamma \oint_{\Gamma_h} h^{-1}(\mathbf{u} \cdot \mathbf{n}_h)(\mathbf{v} \cdot \mathbf{n}_h) \, ds \right| \le C h_{\Gamma}^{3/2}. \tag{62}$$

With our choice of \mathbf{v} , (59) gives

$$\left| \oint_{\Gamma_h} h^{-1}(\mathbf{u} \cdot \mathbf{n}_h)(\mathbf{v} \cdot \mathbf{n}_h) \, ds \right| \ge \left| \oint_{\Gamma_h} h^{-1} |\mathbf{u} \cdot \mathbf{n}_h|^2 \, ds \right| - Ch_{\Gamma}^k \ge Ch_{\Gamma}, \tag{63}$$

provided Γ has a region with non-zero curvature and **u** is sufficiently smooth. Recall that $k \geq 2$. From (57) and (63), we conclude that

$$\|\|\mathbf{u} - \mathbf{u}_{h}^{2}\|\|_{h} \ge C\gamma h_{\Gamma} \|\mathbf{v}\|_{H^{1}(\Omega_{h})} \ge C\gamma h_{\Gamma} (\|\mathbf{u}\|_{H^{1}(\Omega_{h})} - Ch_{\Omega}^{k} \|\mathbf{u}\|_{H^{k+1}(\Omega_{h})}), \tag{64}$$

using (59). This confirms that algorithm 2 is less accurate in terms of mesh size than algorithm 1, but it does not show that the estimates in Theorem 4.4 and Theorem 4.3 are optimal. On the other hand, it does prove that algorithm 2 degenerates as $\gamma \to \infty$.

5.1 Lower bounds for the first algorithm

Lower bounds for $\mathbf{u} - \mathbf{u}_h^1$ are trickier since most of the terms in (29) are of the same order, so it is difficult to know if cancellations occur. However, for smoother $\mathbf{v} \in Z$ satisfying (59), some of the terms in (29) are of smaller order. In particular, the term in (34) can easily be seen to improve to order $h_{\gamma}^{5/2}$ for \mathbf{v} satisfying (59), as in (36). Surprisingly, the final term in (29) is of even higher order, unlike the situation for algorithm 2 where this term is the largest. Replacing (35), we have

$$\left| \oint_{\Gamma_h} h^{-1}((\mathbf{u} - \mathbf{u} \circ \boldsymbol{\pi}) \cdot \mathbf{n}_{\pi})(\mathbf{v} \cdot \mathbf{n}_{\pi}) ds \right| \leq C h_{\Gamma} \|\mathbf{v} \cdot \mathbf{n}_{\pi}\|_{L^{1}(\Gamma_h)} \|\mathbf{u}\|_{W_{\infty}^{1}(\widetilde{\Omega})}$$

$$= C h_{\Gamma} \|(\mathbf{u} - \mathbf{v}) \cdot \mathbf{n}_{\pi}\|_{L^{1}(\Gamma_h)} \|\mathbf{u}\|_{W_{\infty}^{1}(\widetilde{\Omega})} \leq C h_{\Gamma}^{k+2} \|\mathbf{u}\|_{W_{1}^{k+1}(\Gamma_h)} \|\mathbf{u}\|_{W_{\infty}^{1}(\widetilde{\Omega})},$$
(65)

using (59). Recall that this is the term multiplied by γ , so the effect of increasing γ in algorithm 1 is much less than for algorithm 2. Thus we have shown that for \mathbf{v} satisfying (59), the terms (34), (35), and (36) are all higher order.

However, for (31), a new argument is required. We begin with a general estimate.

Lemma 5.1 Suppose that the mesh is non-degenerate [1]. Then

$$\left| \oint_{\Gamma_h} (\mathbf{n}_h - \mathbf{n}_{\pi})^t \mathbf{w} \, ds \right| \le C \sum_{e \in \Gamma_h} \begin{cases} h_e^3 \| \mathbf{w} \|_{W_{\infty}^1(\widetilde{\Omega})} & d = 2 \\ h_e^4 \| \mathbf{w} \|_{W_{\infty}^1(\widetilde{\Omega})} + h_e^3 \| \mathbf{w} \|_{L^{\infty}(\widetilde{\Omega})} & d = 3 \end{cases}, \tag{66}$$

for fixed $\ell \in \mathbb{R}$.

Proof. In two dimensions, $\mathbf{n}_h - \mathbf{n}_{\pi}$ can be written using the notation surrounding (33) for an edge $e = \{(x, 0 : 0 \le x \le h\}$ as

$$(\mathbf{n}_{\pi} - \mathbf{n}_{h})(x) = (1 + \delta'(x)^{2})^{-1/2} (-\delta'(x), 1 - \sqrt{1 + \delta'(x)^{2}})^{t} = \pm \delta'(x) \boldsymbol{\tau}_{h} + \mathcal{O}(h^{2}).$$

Note that $1/C \le h/h_e \le C$ since the mesh is nondegenerate. Therefore

$$\left| \oint_{e} (\mathbf{n}_{h} - \mathbf{n}_{\pi})^{t} \mathbf{w} \, ds \right| \leq \left| \oint_{e} \delta' \boldsymbol{\tau}_{h}^{t} \mathbf{w} \, ds \right| + Ch^{3} \|\mathbf{w}\|_{L^{\infty}(\omega_{h})}. \tag{67}$$

Integration by parts gives

$$\left| \oint_{e} \delta' \boldsymbol{\tau}_{h}^{t} \mathbf{w} \, ds \right| = \left| \oint_{e} \delta \left(\boldsymbol{\tau}_{h}^{t} \mathbf{w} \right)' ds \right| \le C h^{3} \| \mathbf{w} \|_{W_{\infty}^{1}(\omega_{h})}, \tag{68}$$

proving (66) in two dimensions (d = 2). In three dimensions, $\mathbf{n}_h - \mathbf{n}_{\pi}$ can be written on a face $e = \{(\mathbf{x}, 0) : \mathbf{x} \in e\}$ as

$$(\mathbf{n}_{\pi} - \mathbf{n}_{h})(x) = (1 + |\nabla_{2}\delta(x)|^{2})^{-1/2} (-\nabla_{2}\delta(x), 1 - \sqrt{1 + \delta'(x)^{2}})^{t}$$

= $-(\nabla_{2}\delta(x), 0)^{t} + \mathcal{O}(h^{2}).$ (69)

Therefore

$$\left| \oint_{e} (\mathbf{n}_{h} - \mathbf{n}_{\pi})^{t} \mathbf{w} \, ds \right| \leq \left| \oint_{e} (\nabla_{2} \delta(x), 0)^{t} \mathbf{w} \, ds \right| + Ch^{4} \|\mathbf{w}\|_{L^{\infty}(\omega_{h})}. \tag{70}$$

Integration by parts gives

$$\left| \oint_{e} \left(\nabla_{2} \delta(x), 0 \right)^{t} \mathbf{w} \, ds \right| \le C h^{3} \| \mathbf{w} \|_{L^{\infty}(\partial e)} + C h^{4} \| \mathbf{w} \|_{W_{\infty}^{1}(\omega_{h})}. \tag{71}$$

Summing over e completes the proof of Lemma 5.1.

Applying Lemma 5.1 with $\ell = 0$ to $\mathbf{w} = \mathcal{D}(\mathbf{u})\mathbf{v}$ in (31) gives

$$\left| \oint_{\Gamma_h} (\mathbf{n}_h - \mathbf{n}_\pi)^t \mathcal{D}(\mathbf{u}) \mathbf{v} \, ds \right| \le C h_\Gamma^2, \tag{72}$$

in two dimensions. Thus the best lower bound that we can give in two dimensions for the error in Nitsche's method is $\mathcal{O}(h_{\Gamma}^2)$ using \mathbf{v} as in (59).

5.2 Another approach

The term in (29) multiplied by γ is

$$\oint_{\Gamma_h} h^{-1}((\mathbf{u} - \mathbf{u} \circ \boldsymbol{\pi}) \cdot \mathbf{n}_{\pi})(\mathbf{v} \cdot \mathbf{n}_{\pi}) ds.$$
 (73)

Let us evaluate

$$(\mathbf{u} - \mathbf{u} \circ \boldsymbol{\pi}) \cdot \mathbf{n}_{\pi} = \mathbf{u} \cdot \mathbf{n}_{\pi}$$

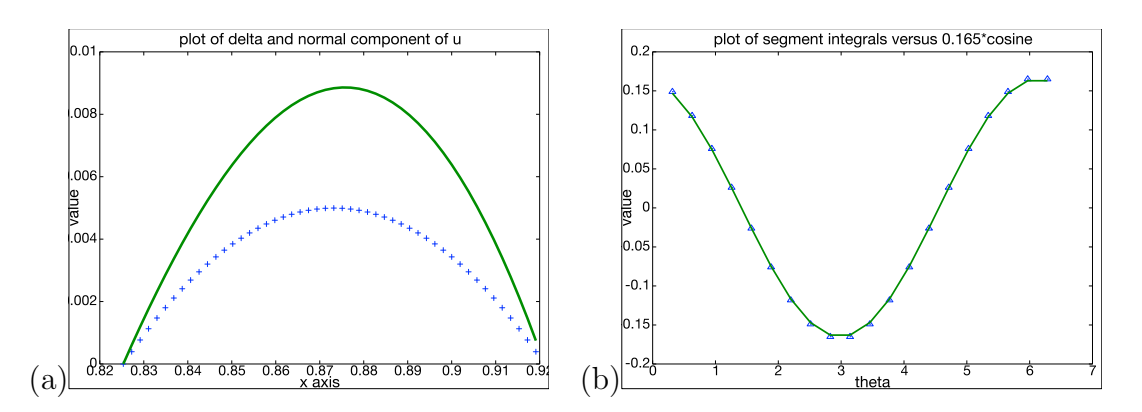


Figure 2: (a) Plot of δ (+'s) and $\mathbf{u} \cdot \mathbf{n}_{\pi}$ for a typical edge e, plotted as a function of the x-coordinate. (b) Plot of segment integrals (74) (indicated by triangles) versus $0.165 \cos \theta$ (solid line); 20 segments corresponding to a fixed angle of 18 degrees.

for potential flow (9) around a cylinder. First, we need to evaluate \mathbf{n}_{π} on Γ_h . For $\mathbf{x} \in \Gamma_h$, we have $\pi(\mathbf{x}) = \mathbf{x} + \delta(\mathbf{x})\mathbf{n}_h \in \Gamma$, where we know from [2] that

$$\delta(\mathbf{x}) = \sqrt{1 - |\mathbf{x}|^2 + (\mathbf{x} \cdot \mathbf{n}_h)^2} + \mathbf{x} \cdot \mathbf{n}_h \,,$$

by using the fact that $|\mathbf{x} + \delta(\mathbf{x})\mathbf{n}_h| = 1$. For $\mathbf{x} \in \Gamma$, $\mathbf{n}(\mathbf{x}) = -\mathbf{x}$. Thus

$$\mathbf{n}_{\pi}(\mathbf{x}) = -\pi(\mathbf{x}) = -(\mathbf{x} - \delta(\mathbf{x})\mathbf{n}_h)$$

for $\mathbf{x} \in \Gamma_h$. Recall from (9) that

$$u_x(x,y,z) = 1 - \frac{x^2 - y^2}{(x^2 + y^2)^2}, \qquad u_y(x,y,z) = \frac{-2xy}{(x^2 + y^2)^2}, \qquad u_z = 0.$$

Consider a segment e of Γ_h between two vertices \mathbf{x}^0 and \mathbf{x}^1 of Γ_h . Then we can write the segment as

$$\mathbf{x}(t) = t\mathbf{x}^0 + (1-t)\mathbf{x}^1, \quad 0 \le t \le 1.$$

Define $(\xi, \eta) = \mathbf{x}^1 - \mathbf{x}^0$. Then

$$\mathbf{n}_h = \frac{(\eta, -\xi)}{\sqrt{\xi^2 + \eta^2}}.$$

In Figure 2(a), we see a plot of $\mathbf{u} \cdot \mathbf{n}_{\pi}$ on a typical edge (solid line) versus δ (+'s). Note that $\mathbf{u} \cdot \mathbf{n}_{\pi}$ is comparable to $\delta = \mathcal{O}(h^2)$. Since we are interested in integrals, we computed

$$\chi(e) = \oint_{c} h^{-3} \mathbf{u} \cdot \mathbf{n}_{\pi} \, ds = \oint_{c} h^{-3} ((\mathbf{u} - \mathbf{u} \circ \boldsymbol{\pi}) \cdot \mathbf{n}_{\pi}) \, ds. \tag{74}$$

In Figure 2(b), the integrals (74) are plotted for a regular approximation Γ_h consisting of 20 segments corresponding to a fixed angle of 18 degrees. Each segment integral is plotted (indicated by triangles) as a function of the angle corresponding to the center θ_e of the

segment e. Remarkably, this curve is closely matched to $0.165 \cos \theta_e$ (solid line), and this match is independent of the number of segments, that is

$$\chi(e) \approx 0.165 \cos \theta_e$$

with the approximation only improving as the number of segments increases. Thus if we could pick $\mathbf{v} \in Z$ such that $\mathbf{v} \cdot \mathbf{n}_{\pi}|_{e} \approx \cos \theta_{e}$ then summing (74) would give

$$\oint_{\Gamma_h} h^{-1}((\mathbf{u} - \mathbf{u} \circ \boldsymbol{\pi}) \cdot \mathbf{n}_{\pi})(\mathbf{v} \cdot \mathbf{n}_{\pi}) ds \approx \sum_{e} h_e^2 \chi(e) \cos \theta_e \approx C h_{\Gamma}.$$
 (75)

Note that $\mathbf{w} = -(1,0)$ satisfies $\mathbf{w} \cdot \mathbf{n} = \cos \theta$ on Γ . Thus we can solve a Stokes problem

$$-\Delta \mathbf{w} + \nabla q = \mathbf{0} \text{ in } \Omega, \quad \nabla \cdot \mathbf{w} = 0 \text{ in } \Omega,$$

$$\mathbf{w} = -(1, 0) \text{ on } \Gamma, \quad \mathbf{w} = \mathbf{0} \text{ on } \partial \Omega \backslash \Gamma.$$
 (76)

Analogous to (59), we pick $\mathbf{v} \in Z$ such that

$$\|\mathbf{w} - \mathbf{v}\|_{H^1(\Omega_h)} \le Ch_{\Omega}^k \|\mathbf{w}\|_{H^{k+1}(\Omega_h)}, \quad \|\mathbf{w} - \mathbf{v}\|_{L^1(\Gamma_h)} \le Ch_{\Gamma}^{k+1} \|\mathbf{w}\|_{W_1^{k+1}(\Gamma_h)},$$
 (77)

using [9]. Then \mathbf{v} satisfies

$$\| \mathbf{v} \|_{\pi} \approx \| \mathbf{w} \|_{\pi} \approx \sqrt{c_1 + c_2 \gamma h_{\Gamma}^{-1}}.$$

Therefore

$$\|\|\mathbf{u} - \mathbf{u}_h^1\|\|_{\pi} \ge C \frac{\gamma h_{\Gamma}}{\sqrt{c_1 + c_2 \gamma h_{\Gamma}^{-1}}} \approx C \sqrt{\gamma} h_{\Gamma}^{3/2},$$

for h_{Γ} sufficiently small.

6 Conclusions

Nitsche's Method can be used effectively to implement slip boundary conditions for Navier–Stokes using the Taylor–Hood approximation with polygonal approximation of curved boundaries. The choice of normal and tangential vectors used in the Navier boundary conditions must be done judiciously, but then mesh refinement at the boundary can mitigate the polygonal boundary approximation. Potential flow provides an exact solution, in both two and three dimensions, to test the implementation of Navier's slip boundary condition.

7 Acknowledgments

We thank Rolf Stenberg for assistance. We thank Tabea Tscherpel for valuable suggestions.

REFERENCES 19

References

[1] Susanne C. Brenner and L. Ridgway Scott. The Mathematical Theory of Finite Element Methods. Springer-Verlag, third edition, 2008.

- [2] T. Dupont, Johnny Guzmán, and L. R. Scott. Obtaining full-order Galerkin accuracy when the boundary is polygonally approximated. *TBD*, 2021.
- [3] Vivette Girault and Pierre-Arnaud Raviart. Finite Element Methods for Navier-Stokes Equations. Springer Series in Computational Mathematics, volume 5. Springer-Verlag, Berlin, 1986.
- [4] Ingeborg Gjerde and L. Ridgway Scott. Kinetic-energy instability of flows with slip boundary conditions. *Journal of Mathematical Fluid Mechanics*, submitted:21, 2021.
- [5] Ingeborg Gjerde and L. Ridgway Scott. Nitsche's method for Navier-Stokes equations with slip boundary conditions. *Mathematics of Computation*, accepted:31, 2021.
- [6] A. Logg, K.A. Mardal, and G. Wells. Automated Solution of Differential Equations by the Finite Element Method: The FEniCS Book. Springer-Verlag New York Inc, 2012.
- [7] Chiara Neto, Drew R. Evans, Elmar Bonaccurso, Hans-Jürgen Butt, and Vincent S. J. Craig. Boundary slip in Newtonian liquids: a review of experimental studies. *Reports on Progress in Physics*, 68(12):2859, 2005.
- [8] L. Ridgway Scott. *Introduction to Automated Modeling with FEniCS*. Computational Modeling Initiative, 2018.
- [9] L. Ridgway Scott. A local Fortin operator for low-order Taylor-Hood elements. Research Report UC/CS TR-2021-07, Dept. Comp. Sci., Univ. Chicago, 2021.
- [10] R. Scott. Interpolated boundary conditions in the finite element method. SIAM J. Numer. Anal., 12:404–427, 1975.
- [11] V. Thomee. Galerkin Finite Element Methods for Parabolic Problems. Springer Verlag, 1997.